Mixed-Valent Compounds and their Properties - recent Developments

Jean-Pierre Launay

Title: Mixed valence compounds and their properties. Some recent evolutions.

Author : Jean-Pierre Launay, Université de Toulouse, CEMES-CNRS, 29 rue Jeanne Marvig, 31055 Toulouse, France

Abstract

Recent evolutions, essentially in the last 15 years, are reviewed in the field of molecular mixed valence compounds and their properties. The considered systems are of the type M_n – BL - M_n where M_n is either a monometallic terminal site (n = 1) or a polymetallic cluster (n = 2, 3), and BL is a bridging ligand. A large variety of bridging ligands is considered: non-innocent, long conjugated, ambidentate, cross-conjugated, switching.

The theoretical descriptions are briefly reviewed and sorted according to their degree of complexity/accuracy: simple orbital models, modified Marcus-Hush diagrams, 3D diagrams with two nuclear degrees of freedom, and finally quantitative models (mainly from DFT) with geometrical optimization. With improved DFT functionals, the prediction of the class II or III nature of a symmetrical complex can now be addressed.

1. Introduction

In the field of Coordination Chemistry, mixed-valence compounds; that is compounds in which a given element is present in different oxidation states, represent a unique opportunity to study the most fundamental aspects of intramolecular electron transfer. They have been the subject of a large number of papers in the last decades, and their properties are summarized in many comprehensive reviews.[1] Indeed they allow particularly clear investigations combining synthetic chemistry, physicochemical characterizations (mainly spectroscopic), and finally theoretical and computational studies. Although the investigated intramolecular process – an electron exchange between two parts of a molecule- appears very simple, it can manifest under very different aspects, because the electronic motion is generally coupled to a change in geometry; that is nuclear motions.

In this minireview, we consider recent advances in the field, by focusing on the results published in the last 15 years. Without neglecting the importance of synthetic elaboration, we emphasize the problem of the electronic structure description, with the associate machinery of theoretical computations. To make the analysis simpler (if possible !) and also save much space, we consider mainly the archetypical structure of the M_n – L – M_n type; that is two metal atoms (n = 1), or small clusters (n = 2 or 3) linked by a bridging ligand (Figure 1). Thus important aspects of mixed-valence chemistry will not be considered, although they would by themselves deserve a specific review. The reader can consult recent reviews on these topics, in particular reduced polyoxometallates,[2] complex multimetallic or high-nuclearity structures[3], dendrimers[4], polymers and chain compounds.[5] Regarding the metal nature, we describe only systems with transition metal ions (due to the richness of their oxidation states), with a short incursion towards mixed-valence organic compounds.

2. The standard 2-state model

The standard 2-state model emerged at the end of the ‘60’s, from the contributions of R. Marcus, N. S. Hush, P. Day.[6] It is conceptually the simplest, because the structure is reduced to two localization sites, one with the lowest oxidation state (donor) and the other with higher one (acceptor), and the problem appears in its purest form when the two sites are chemically equivalent. We recall briefly its basic features.

The model describes electron transfer from potential energy curves of the total system as a function of a nuclear coordinate Q defining the changes in both the inner (intramolecular bond lengths) and outer (state of the solvent polarization) coordination spheres (Figure 2). Two potential energy curves are considered, corresponding to the two limiting electronic configurations, for instance $Ru^{II} – Ru^{III}$ and $Ru^{III} – Ru^{II}$ for the emblematic Creutz-Taube ion[] and similar compounds. They correspond to a completely localized picture and can be called “diabatic” states. The Q coordinate is an asymmetric combination of coordinates localized on each sub-unit, so that Q = 0 corresponds to a right-left symmetrical situation while $Q \neq 0$ corresponds to situations where the right site is adapted to one oxidation state and the left one to the other. The dependence of the energies upon Q is quadratic (harmonic oscillator approximation) and the minima are symmetrically disposed around Q = 0. The λ reorganization parameter is linked to the change in bond lengths and solvent molecules positions when the two oxidation states are swapped. In this review, we shall consider mainly the case where the two possible configurations have the same energy.

The two unperturbed parabolas are valid descriptions in the limit of no electronic interaction between the sites, *i.e.* when the wave function of the extra electron is fully localized either on the right or the left site. However interesting compounds are those for which there is an electronic interaction deriving from overlap between orbitals accommodating the extra electron on either site. This electronic interaction, denoted here V_{ab}, mixes the electron wavefunctions and decreases the total energy of the system, because the extra electron is now in a more stable orbital. (Note that this simplified explanation favors the frequent confusion between one-electron energy and total potential energy). For simplicity, in the following, we consider V_{ab} as a positive quantity, but the true quantity involved in quantum chemical calculation is a resonance integral, which is negative.
As usual in quantum chemistry, the effects of electronic interaction are larger when the two initial levels are closed, thus in the crossing region of the potential energy curves.

From this simple arguments, a straightforward calculation based on the solution of a 2×2 determinant shows three different cases, corresponding to the three famous classes introduced by Robin and Day.[6c] If V_{ab} is very small, the starting parabolas are unchanged and no electron transfer occurs (class I); if V_{ab} is increased, deviations from the parabolas appear, first in the crossing region, and give rise to adiabatic states. According to the value of V_{ab} compared to λ, two minima are still observed (class II, $V_{ab} < \lambda/2$) or only one (class III, $V_{ab} > \lambda/2$). In class II, the electron is mainly localized on one site, but a thermally electron transfer is possible, while in class III, the electron is fully delocalized. The compounds evoked in the Review are essentially class II or III. Note that the experimental distinction between classes II and III must take into account the time scale of the used method (for a short presentation, see section 3.2.2.5 of ref[1h]).

In class II or III compounds, a vertical optical process is possible, the so-called “intervalence transition”. For a class II system, its energy is λ, corresponding to a genuine electron transfer between the two sites (although this statement must be tempered by the fact that there can be an appreciable degree of ground state delocalization). For a class III system, the energy is $2\,V_{ab}$, and the transition has no longer a charge transfer character; it is actually a transition between orbitals equally delocalized on the two sites, but with different symmetries. Intervalence transitions allow the determination of V_{ab}, the degree of electronic coupling between sites. For class III, it is merely one half of the energy of the transition; for class II, it can be obtained from Hush’s formula:

$$V_{ab} = \frac{2.05\,10^{-2}\sqrt{\bar{\nu}\,\Delta\bar{\nu}_{1/2}\,\varepsilon_{max}}}{R_{MM}} \qquad (1)$$

where $\bar{\nu}$ is the energy of the transition, ε_{max} its maximum extinction coefficient, $\Delta\bar{\nu}_{1/2}$ its full width at half-maximum, and R_{MM} is the metal-metal distance. Despite the difficulty raised by

the R_{MM} distance which can be markedly different from the geometrical distance when the degree of ground state delocalization is important, this equation is widely used in practice.

Other ways of quantifying the electronic interaction exist. One of the most popular is the wave splitting between consecutive electrochemical processes, exploiting the fact that after a first reduction (oxidation) of a mixed valence compound, the second electron (hole) is usually more difficult to introduce. But this wave spitting depends on a number of factors and not only on the electronic interaction. There are good reasons to be careful about the use of this indicator.[1a, 7] whose only advantage is its ease of measurement. It can be used, at a pinch, in specific cases on a homologous series of complexes, after careful calibration.

An important issue is the rate of decay of V_{ab} with distance, as it concerns the possibility to transfer electrons across organic fragments, in the general challenge of Molecular Electronics. Usually, this decay is described by an inverse exponential law:[1a, 1h, 8]

$$V_{ab} = V_{ab}^{0} \exp(-\beta R_{MM}) \qquad (2)$$

where β (in $Å^{-1}$) is hoped to be as small as possible. Many efforts are devoted to the search of deviations (in the good direction !) with respect to this law.

The 2-state model suffers, by construction, of several weaknesses. First, the separation of the whole molecule into a donor and an acceptor site can be be artificial and too much based on chemical intuition, neglecting in particular the covalent nature of the intramolecular links. Second, it does not take into account explicitly the bridging ligand. Its influence is only reduced to the determination of the V_{ab} electronic coupling parameter, which becomes an effective parameter. As will be seen below, more complete treatments exist, but are much more complex to use. Thus the 2-site model keeps its status of an inescapable starting point for the description of a new system.

3. Some original structures

3.1. Special terminal sites

There has been a huge diversity in mixed valence chemistry with metal end groups. Among them, we select (somewhat arbitrarily !) some particular end groups made of one or several metal atoms.

Cyclometallated terminal sites. Many mixed valence compounds have been prepared with a cyclometallated terminal site, comprising a metal-carbon σ bond.[9] A typical example involves a deprotonated phenypyridine moiety and a ruthenium atom (Figure 3). This structure derives formally from the famous $[Ru(bpy)_3]^{2+}$ (bpy = 2,2' bipyridine) structure by replacement of the nitrogen atom of a bipyridine by a carbon atom, with a concomitant apparition of an extra negative charge on the ligand. Another frequently used structure derives from terpyridine by substitution of a nitrogen atom either on the central pyridine or on the lateral ones (Figure 3).

In cyclometallated complexes, since carbon has orbitals of higher energy than nitrogen, thus closer to the metal orbitals, the metal-carbon bond is more covalent. The increased mixing between metal and ligand orbitals increases the electronic coupling between remote metal atoms.[10] But in addition, for ligands derived from terpyridine, the effect is sensitive to the position of the carbon atom, more coupling being observed when the carbon is on the central sites rather than on the lateral sites.[9b] An advantage of cyclometallated systems derived from terpyridine is the intense and well resolved intervalence transitions.

Cyclometallated end groups have allowed the study of intramolecular electron transfer in a large variety of structures. The subject has been extensively reviewed by Zhong in 2016[9b] and we just quote the main studied points: the role of various groups intercalated in the bridge structure such as thiophene or anthracene (the latter being particularly efficient), the possible use of NMe_2, PPh_2, triazole or benzimidazole as lateral ligands replacing the external pyridines in the structure of terpyridine, the distance dependence of the electronic coupling in a series of homologous ligands of increasing length.

Recently, cyclometallated systems allowed the study of electron transfer through ligands containing a redox active amine bridge whose donor properties can be modulated by proper substitution.[9c]

M_2(acetate)$_4$ (M = Mo, W) terminal sites.[11] These sites belong to the general $M_2(acetate)_4$ structure, where the two metal atoms in formal oxidation state II (d^4) are linked by a quadruple bond corresponding to the $\sigma^2\pi^4\delta^2$ filling. The overall shape is that of a paddlewheel (Figure 4a). If one acetate is replaced by a bridging ligand like oxalate, it is possible to link the two M_2 subunits. The δ orbitals mix together but indirectly through interaction with an oxalate π^* orbital. One-electron oxidation generates a mixed valence form in which a hole must be shared between the two M_2 terminal sites.

The great attractiveness of these complexes resides in the simplicity of the intervalence spectrum. The MO diagram shows that the δ orbital of a M_2 unit is well separated from others. Thus in the mixed valence dimer of M_2 units, the intervalence band is not plagued by overlap with other types of transitions.

Extensive studies have been performed on systems with Mo, W or a combination (a Mo_2 and a W_2 site) and various bridges (oxalate, substituted terephthalate, etc…). In addition to intervalence transitions, one can measure EPR spectra which exhibit an hyperfine structure due to interaction of the unpaired electron with ^{95,97}Mo (I = 5/2, 6 hyperfine lines if localization on one atom) or ^{183}W (I = 1/2, 2 hyperfine lines). The electronic interaction is generally strong and most systems are delocalized (class III) even for long ligands such as terephthalate. The metal nature is important, stronger couplings being observed with W rather than Mo,[11c] which is probably due to the larger spatial extension of 5d orbitals. A detailed study of oxalate-bridged systems shows the importance of considering the metal-to-ligand charge transfer transition (MLCT) in addition to the intervalence transition, because both are influenced by the LUMO of the bridge.[11b] This is a strong argument in favor of a three-state model taking into account explicitly the bridging ligand (see section 4.1). Then, exploiting the logic of the model, it is possible to consider a symmetric nuclear coordinate (see below) along which an electron transfer occurs with the bridge. By analogy with the two-state model, the potential energy curve along this direction could exhibit 1 ou 2 minima, and Chisholm propose to call Class IV the compounds for which there is strong delocalization, i.e. one can evolve continuously without energy barrier between a metal-localized hole towards a bridge-localized hole. The denomination “class IV” emphasizes the “more-than-class-III” character of delocalization.[11b]

M_2ap_4 sites. While in the previous systems, the bridge was connected side-on to each terminal M_2 unit, in M_2ap_4 structures (M = Ru, ap = 2-anilinopyridinate) it is connected end-on, *i.e.* along the axis of the paddlewheel (Figure 4b). The M_2ap_4 unit consists in two ruthenium atoms held together by four deprotonated anilinopyridine ligands and a metal-metal bond.[12a] This unit is usually linked to the ethynyl end of a bridging ligand (bearing formally a negative charge). Thus the average oxidation state of ruthenium is 2.5, corresponding to a class III mixed valence system inside the M_2ap_4 unit. The bond order of the metal-metal bond is 2.5, and the spin state of the M_2ap_4 unit is S = 3/2.[12a] The M_2ap_4 terminal unit can be efficiently combined with all-carbon bridging ligands of the polyyne-diyl type. As will be seen below, the corresponding mixed-valence systems allow the study of long distance electron transfer along the polyyne-diyl chain, as well as the effects of cross-

conjugation. Another interesting property of the Ru_2ap_4 unit is their extreme stability upon redox cycling, up to billion cycles, allowing their use in a demonstrator of a nanowire flash memory.[12b]

Ru_3O terminal sites. The triangular cluster $[Ru_3O(acetate)_6(CO)L_2]$ (abbreviated as Ru_3O), where L is a nitrogen-donor ligand constitutes a particularly appealing terminal site.[7a,13] It is very stable, the Ru atoms being linked by acetate bridges and a central oxide ion (Figure 5). The ruthenium atoms are formally in oxidation states III, III, II, although they are electronically equivalent. One of the L ligand can be a bridging ligand (1,4 pyrazine, 4,4'-bipyridine), the other an ancillary ligand with various donor properties (pyridine, dimethylamino pyridine, cyanopyridine), while CO can be used as a "marker" thanks to its infrared band. Upon electrochemical reduction, monoelectronic waves are obtained, allowing the preparation of a mixed valence form in which one of the trimeric clusters has been formally reduced. It can be written as $Ru_3^{III,III,II}$ – BL - $Ru_3^{III,II,II}$ (BL = Bridging Ligand), the real question being to know the state of delocalization between the two Ru_3O moieties. An intervalence transition corresponding to an *intramolecular intercluster* process is observed near 11 000 cm^{-1}, but partly overlapped by a lower energy *intracluster* transition.

The great interest of these systems is that the ν(CO) band is sensitive to the oxidation state of the trimeric cluster. Thus very complete studies are possible by varying the bridging ligand, the ancillary ligand, the solvent, etc… The ν(CO) band is either spilt when the two clusters are inequivalent in the IR time scale, or unique if the intramolecular exchange is fast, and by Bloch-type line shape analysis, it is even possible to determine the rate of intramolecular intercluster electron transfer, which is in the 10^{11} s^{-1} range. Such a high rate suggest that these complexes are at the class II / class III borderline, a category introduced and defined by Meyer in 2001.[1b] In this new class, a tiny influence, such as a change of solvent, can drive the system from a localized to a delocalized behavior. A possible definition of the class II-III system is that the exchanging electron and the nuclear coordinates are localized (as in class II), but the solvent coordinates are delocalized (as in class III).[1b]

Returning to the case of mixed valence with Ru_3O sites, studies of the role of solvent at different temperatures show that the rate of electron transfer does not correlate with *thermodynamic* properties of the solvent (as suggested by the original Marcus-Hush theory using optical and static dielectric constants), but correlates with its *dynamic* properties, like solvent reorientation frequency.[13]

Additional studies on these systems have been performed by Raman resonance showing the role of the bridging ligand, and are discussed later in 4.1.

3.2. Some particular bridging ligands

Non-innocent ligands. Many authors have pointed out that efficient bridging ligands for electron transfer are those for which there is an appreciable degree of covalency, *i.e*. some mixing of the metal and ligand wavefunctions. When this effect becomes important, it is more and more difficult to assign a definite oxidation state to the metal, and consequently to define the exact state of the ligand. Non-innocence is thus the power of such ligands to prevent not only writing the structure as made of parts with an integral charge, but also in some cases writing a simple and unique Lewis form for the ligand itself.

The most common aspect of "non-innocence" is provided by redox-active ligands, as they can exist by themselves under different forms (Figure 6). Considerable work in this area has been achieved by Kaim and Lahiri,[14] to answer the following question: if we reduce (or oxidize) a binuclear homovalent form, does the redox process concern the metals or the bridging ligand? The answer necessitates a judicious combination of several techniques. Note that the presence of an absorption band in the near-IR is not a reliable criterion since oxidized or reduced form of an organic ligand can present bands in this range which can be

mistakenly interpreted as intervalence transitions. EPR on the other hand can yield valuable information since organic radicals usually present a sharp signal near g = 2.0, while metal-based paramagnetic species present much broader signals with g appreciably different from 2.0.

A typical example is represented by 1,4-dicyanamidobenzene complexes, first studied by Crutchley (Figure 7a).[15] Several ruthenium binuclear complexes have been prepared, and let us consider the case of a ruthenium(II) homovalent form. As dicyanamidobenzene is a formally negative ligand, the initial electronic structure can be written Ru^{II} – ($dicyd^{2-}$) – Ru^{II}. But upon one-electron oxidation, since $dicyd^{2-}$ can be easily oxidized as anion-radical, one could formulate the product either as a Ru^{II} – ($dicyd^{2-}$) – Ru^{III} (type A on Fig. 6) mixed valence compound (without prejudging of its class II/III nature) or as a Ru^{II} – ($dicyd^{\circ-}$) – Ru^{II} (type B) homovalent one bridged by an anion-radical. Actually both possibilities can exist according to the compounds and experimental conditions. Thus with acac and terpy as ancillary ligands, formulation B is privileged[16], and this is also the case with terpy and bipy.[17b] But for the ruthenium(pentaammine) forms initially studied by Crutchley and reinvestigated by Kaim, Crutchley *et al,* the results are more ambiguous. Experiment suggests the A formulation, while theory (DFT) suggests B.[17a] Refining the calculations with advanced descriptions of the solvent reveals that the solvent influence could change the balance between A and B.

Note that IR studies show that oxidation of a Ru^{II} site to Ru^{III} has consequences on the balance between the possible mesomeric forms of the cyanamido end (Figure 8a). This evolution will be encountered below in carbon-rich bridges.

We considered above the case of a ligand which can be easily oxidized. The converse example is provided by systems bridged by quinonoidal neutral bridges which can be easily reduced as anion-radicals. Thus starting from the $(acac)_2Ru^{III}$ (BL) $Ru^{III}(acac)_2$ system (where BL is a tetraazapentacenequinone), the one-electron reduced form can be written either as Ru^{II} – (BL) – Ru^{III} or Ru^{III} – ($BL^{\circ-}$) – Ru^{III}.[18] Here again there is a discrepancy between experiment (EPR suggesting a metal-centered spin) and theory (DFT suggesting spin density on the ligand). (In addition, the comparison depends on the exact linkage isomer). It is likely that both electronic structures forms have very close energies.

In the previous examples, “non-innocence” originated from the redox-active character of the ligand. Another type of “non-innocence” is encountered with organometallic end groups and carbon-rich bridges. The subject has been reviewed and well explained elsewhere.[19] Typical examples imply organometallic moieties of the type MCp*(dppe) or $ClM(dppe)_2$ linked by a sigma bond to a polyalkynyl bridge. Here, since the metal-carbon bond is essentially covalent, when oxidation is performed, there are few consequences on the actual charge distribution between the metal and ligand, but rather on the pattern of single and multiple bonds (Figure 8b). Oxidation favors the cumulene resonant form with respect to the polyalkynyl form, an effect similar to the one observed with dicyanamidobenzene.[17b] The competition between the polyalkynyl and cumulene forms has be studied by a range of physical methods (EPR, IR, UV-vis,…) as well as theoretical methods (DFT),[19a] the last one allowing the calculation of equilibrium ligand bond lengths.[19c]

A more pronounced example of bridging ligand modification is provided by the curious mixed valence compound obtained from a dinuclear niobium compound with an inverted sandwich structure in which niobium atoms are bridged by a benzene in a μ-η^6:η^6 way.[20] The formal oxidation state of Nb can be defined as III (d^2). Upon one-electron oxidation, a mixed valence Nb compound is obtained. The electronic structure is described as ($4d^1$) – neutral arene – ($4d^2$), thus oxidation has occurred on the metal, Thanks to the nuclear spin of Nb (9/2), it is possible to exploit the rich hyperfine structure of the EPR spectrum, showing that an unpaired electron is mainly localized on one Nb, but with a smaller contribution from the other, a result typical of class II. But the puzzling fact is that the ligand has completely

changed in geometry and bonding mode. It is now non-planar and linked in a μ-η^2:η^4 mode. Theoretical calculations suggest that the oxidized niobium is the one linked in the η^4 way.

Long all-carbon bridging ligands. These ligands presenting several conjugated ethynyl bonds have been the subject of intense study since 2000. Several reviews can be found in[19d,21]. Among the most recent results, we quote here the case of *bis*(Ru_2ap_4) linked by conjugated triple bonds with one to 9 triple bonds, corresponding to distances of 5 to 25 Å between M_2 units.[22] Mixed valence species are obtained by either reduction or oxidation, and intervalence bands are observed, from which the electronic coupling V_{ab} can be obtained. The exceptional range of distances allows the determination of the rate of decay of V_{ab} with distance for the $1e^-$ reduced species. The β attenuation factor is found as 0.15 $Å^{-1}$, which is slightly higher than for other systems with conjugated double bonds giving β near 0.1 $Å^{-1}$.[1a] Thus conjugated triple bonds appear less efficient than conjugated double bonds, a conclusion which emerges also from the theoretical study of the conductance of molecular wires connected to electrodes.[23]

Another consequence of the exceptional number of triple bonds is the possibility to study the effect of cycloaddition/insertion in the chain by a molecule such as $Co_2(dppm)(CO)_4$ or TCNE. With the Co_2 molecule, the electronic coupling between Ru_2 terminii is reduced, and with TCNE, it is completely suppressed.[24]

Long dicyanamido-type ligands. The 1,4-dicyanamidobenzene structure can be extended by replacing the central benzene ring by biphenyl, biphenylacetylene, biphenyldiacetylene or bis(phenylethynyl)anthracene (Figure 7b).[25] With ruthenium(acac)(terpy) end groups, binuclear Ru^{II} complexes are obtained, for which the oxidation bears on ruthenium (not the bridging ligand). It is thus possible to generate mixed valence Ru^{II}-Ru^{III} species, and on further oxidation homovalent Ru^{III}-Ru^{III} species. As shown by Bonvoisin,[25] the interest of this series is the possibility to measure the V_{ab} electronic coupling on the mixed valence forms and also the magnetic exchange coupling parameter J on the homovalent forms. The comparison between the decay laws of these two parameters is discussed in [25].

Ambidentate ligands. The ambidentate ligand cyanide CN^- has not finished being implemented in new structures, for example cyanide-bridged molecular squares with various metals.[26] Let us recall that in the famous Prussian blue solid and its derivatives, cyanide acts as a bridging ligand between iron(II) and iron(III). The two ends of the ligand behave in a different way, because in these structures, the carbon atom is linked to a low spin Fe^{II}, while nitrogen is linked to a high spin Fe^{III}. The C end generates thus a higher ligand field than the N end.

The trinuclear ruthenium compound $[Cp^*(dppe)Ru^{II} – (\mu\text{-}NC) – Ru^{II}(dmap)_4 – (\mu\text{-}CN) – Ru^{II}(dppe)Cp^*]^{2+}$ where dmap = dimethylamino pyridine and cyanide is linked by *carbon* to the central ruthenium, has been prepared by Sheng *et al*, together with the linkage isomer where the bridging cyanides are linked by *nitrogen* to the central ruthenium.[27a] Upon oxidation of the first isomer, the terminal rutheniums are oxidized first and the one-electron product present a sharp band at 5000 cm^{-1}, assigned to an intervalence band between the outer ruthenium atoms. The system would be a class III system with extensive delocalization on all the trimetallic squeletton. By contrast in the other linkage isomer, it is the central ruthenium which is oxidized first. A mixed valence form is also obtained by one-electron oxidation. The intervalence occurs between one of the outer ruthenium(II) and the central ruthenium(III), at a higher energy than before (8800 cm^{-1}), because of the asymmetry. Note that in the two complexes the oxidation state distribution is the same as in Prussian Blue, that is Ru^{II} linked to carbon and Ru^{III} to nitrogen.

A similar situation was encountered in the earlier trimetallic system $[Cp(dppe)Fe^{II} – (\mu\text{-}NC) – Ru^{II}(phen)_2 – (\mu\text{-}CN) – Fe^{II}(dppe)Cp]^{2+}$ where phen = orthophenanthroline.[27b] There

are two possible isomers, *cis* and *trans*, corresponding to the disposition of the cyanide ligands on the central metal. Here also, the outer metals are oxidized first. For both isomers, an intervalence band is observed for the monooxidized species. DFT calculations show that it is not a simple Fe^{II} to Fe^{III} transition, but rather a transition from an orbital delocalized between Fe^{II} and Ru^{II} towards a Fe^{III} orbital.

Cross-conjugated ligands. Many efficient ligands able to transfer electronic interactions are conjugated, *i.e.* they present an alternation of single and multiple bonds. Typical examples are α,ω bipyridylpolyenes or polyynes. In cross-conjugated ligands, the situation is a first sight similar, but a careful inspection reveals that the electron transfer path contains somewhere a succession of two formally single bonds. Typical examples are penta-1,4-diyn-3-one[28a] or geminal-diethynylethene[28b, 28c, 28d] (Figure 9). (One can remark that the number of carbon atoms constituting the bridge is odd). Metal moieties of the type Cp*(dppe)Ru or $Ru_2(Xap)_4$ (see above) have been attached to both ends of such ligands. It is found either experimentally (generation of a mixed valence form not presenting Intervalence Transition) or theoretically (DFT calculation) that the electronic interaction between the end sites is very small, much less than for a conjugated system of similar length. The effect of cross-conjugation (and even hyperconjugation through a sp3 carbon or silicium) is similarly found in organic mixed valence compounds.[28e]

The orbital interpretation of the weak efficiency of cross-conjugated system to transmit electronic interaction relies on a cancellation of effects when the metal orbitals are mixed with bridge orbitals. Thus it is intimately connected to the modern and broader concept of “quantum interference”. For example, the well-known difference between *meta* and *para* substitution effects in a benzene ring can be related to a destructive quantum interference in the case of the meta connection, and this can be experimentally shown in some mixed valence compounds.[29a, 29b] Quantum interference is expected to play a role in the design of a molecular transistor.[29c, 29d] But the concept has its best range of usefulness in the study of nanojunctions, where a single molecule is linked to two electrodes.[30] When destructive interference occurs between two electronic paths, it manifests as “antiresonance” with a sharp dip in the conductance.[30a]

Switching ligands. The control of electron transfer by an external perturbation is a topic of paramount importance for Molecular Electronics. In this context, mixed valence systems provide a benchmark for the test of molecular structure, because the bridging ligand plays a key role in the intramolecular electron transfer. The simplest implementation makes use of light as a control parameter, and the topic of switchable mixed valence has been recently reviewed by Wenger.[31a] We only recall some important points.

Many chemical structures can present both photoswitching ability and bridging properties for incorporating in the mixed valence structure. One can quote alkenes (*cis-trans* isomerization), norbornadienes (isomerization to quadricyclanes), dimethyldihydropyrenes (isomerization to cyclophanedienes). But the most studied in the recent years is based on the dithienylethene moiety (Figure 10). This fragment has indeed very interesting properties: reversible switching between an open (OFF) and a closed (ON) form is possible at different wavelengths, the isomers are stable and present different electronic properties. In particular, while the closed form exhibits a conjugated pathway between both ends, in the case of the open form, there is only cross-conjugation between the external thiophene groups, which blocks or reduces considerably the electron transfer. Finally, these large changes in electronic communication between extremities are obtained with limited geometrical motion, allowing the inclusion in a compact or solid-state structure.

Many end groups have been used to probe the electron transfer across the structure: cyclometallated Ru(bpy)(pp) where pp = phenylpyridine,[31b] $M(Cp^*)L_2$ groups (M = Fe, Ru, L = CO, phosphine),[31c] $ClRu(dppe)_2$,[31d] The electronic interaction is best probed by the presence/absence of an intervalence transition in the two forms, but in some cases, it is only possible to use the comproportionation constant Kc (from the wave splitting), which is a

measure of the thermodynamic stability of the mixed valence from with respect to a mixture of the homovalent form. Anyway, there is now general consensus to consider this system as an excellent photoswitching fragment. But for the particular case of ferrocene end groups, the photoconversion of the switching unit is strongly perturbed and deactivated due to a multitude of energetically close excited states coming from ferrocene.[31e]

In addition to photoinduced switching, dithienylethenes can be manipulated by oxidation/reduction. In fact the closed form can be reopened by oxidation.[31d] A simple rationale is that oxidation depopulates the HOMO, as in the photochemical process (without of course populating the LUMO). The process can also occur also in the reverse direction, depending on the sêcific molecule. Note that for the free dithienylethene, the oxidation-induced reopening reaction can be extremely efficient in solution owing to a chain reaction mechanism.[31f] When metal atoms with their own redox activity are attached, the behavior can become very complex. Thus with ferrocene end groups oxidation of ferrocene triggers an electrocatalytic ring reopening.[31g]

With $MCpL_2$ (M = Fe, Ru; L = CO or phosphine) end groups, photo-and electro-chromism are observed. In particular the ring closure can be activated either by light or by oxidation followed by reduction, the latter process being even possible for a photochemically inert compound.[31c] The electronic communication was estimated through the comproportionation constant, this procedure being justified by a correlation between Kc and the electronic coupling.[31h] Such systems constitute dually stimuli-responsive molecular switches. More complex associations of stimuli, for instance coordination, redox, guest-binding, are possible.[32]

4. Theoretical descriptions

We encompass in this section several types of descriptions going beyond the standard 2-state model. They aim at several goals : (i) take into account the extensive delocalization between the different parts of the system, in particular when non-innocent bridging ligands are involved; (ii) achieve an accurate description of the electronic and geometrical structure, in particular for systems at the frontier between classes II and III; (iii) explain and reconcile the various measurements: intervalence transitions, but also other properties, taking into account the times scales of the experimental methods.

Broadly speaking, two kinds of descriptions have been practiced in the last years. First, “simple” semi-quantitative descriptions based on monoelectronic orbital models, which can be considered as extensions of the 2-state model, because the starting point is to divide the system into chemically significant parts. Second, more complete quantitative models using advanced quantum mechanical methods, in which the structure is considered as a whole.

To illustrate the discussion on the different models, Figure 11 schematizes the progression from simple monoelectronic models to advanced ones aiming at calculating all properties and elucidating the ground state geometry.

4.1. Semi-quantitative pictorial models

In the frame of the first approach, one can take into account more completely the electronic influence of the bridging, or even ancillary, ligands. Approximating the total electronic energy of the system by the sum of the filled orbital energies, one can elaborate one-electron diagrams, with not only the outer sites orbitals, but also a crucial orbital localized on the bridge (HOMO or LUMO), and in some cases orbitals based on the ancillary ligands.

Thus, to describe mixed valence systems of the type Ru_3O – bridge – Ru_3O, where bridge = typically pyrazine or 4,4’-bipyridine, Kubiak uses a qualitative molecular orbital

scheme (of the type shown on Figure 11a) with one dπ* orbital on each terminal Ru_3O cluster and a π* orbital (LUMO) on the bridge, the diagram accommodating one electron.[13] If the system has a symmetrical ground state structure (class III), the lowest possible transition ("intervalence") is thus from a bonding (cluster-pyrazine-cluster) orbital to non-bonding (out-of-phase cluster) combination. This transition is allowed by symmetry, but since only the lowest orbital has a contribution from the bridge, this "intervalence" transition has some character of a bridging-ligand-to-metal transition. This 3-orbital model shows the importance of overlap at the bridge-cluster junction, but also the role of the energy difference between cluster orbital and bridge LUMO. A more complete description uses a 5-orbital diagram, by adding one ancillary ligand orbital at each end of the system.[13] This predicts the splitting of the "intervalence" transition in two components, which has been observed. The 3-orbital model is also supported by Raman resonance experiments performed on the mixed valence forms. Thus for a complex with two Ru_3O sites bridged by pyrazine, excitation on the intervalence transition exhibit Raman resonance bands which testify of the partial population of the π* (LUMO) of the bridging ligand.

The advantage of such models is to introduce in a natural way the effect of non-innocent ligands. One has however to define in a pertinent way the fragments used in the analysis, for instance metal and ancillary ligands on one hand, bridging ligands on the other hand, with their own frontier orbitals.

Adding extra monoelectronic levels solves however only a part of the problem, the electronic one. Actually, any change in the electronic structure has consequences on the geometrical structure (the nuclear problem). This leads to 3-state models, in which it is the potential energy of the complete system which is plotted (like in Marcus-Hush curves). These models introduce explicitly the bridging ligand, and have been elaborated under different forms.

A first idea is to keep the general E = f(Q) diagram (Figure 11b and 11c) and just add an additional curve representing the situation where the bridging ligand has been oxidized (or reduced). For symmetry reasons, its minimum occurs for Q = 0. This has been used by several authors,[11b, 19d, 33] for the metal-ligand-metal case, but also for trimetallic systems.[34] This allows a first discussion by stressing the existence of an extra electronic state. However, since a third electronic state has been added, there are certainly additional nuclear degrees of freedom. Taking at least one of them into account leads to 3D diagrams in which the potential energy is plotted as a function of *two* nuclear coordinates,[35] and the parabolas of the 2-state model are replaced by paraboloids (Figure 11d).

Three-states models of this type have been introduced between 1984 and 2007 by Ondrechen,[36] Bersuker- Borshch-Chibotaru,[37] Lambert,[38] and Launay.[39] Note that the Lambert model has been devised for *organic* mixed valence systems, with end groups of the triphenylamine type, but since there is a close analogy with inorganic systems, it is wise to consider it in this review. The Launay model is similar, but simpler as it uses less parameters[39]. In these models, the 3D nature of the diagrams allows excursions on potential energy surfaces, illustrating in particular the distinction between a one-step superexchange process (the electron moves directly from one site to the other without residing on the bridging ligand), and two-step hopping process (there is an intermediate reduction or oxidation of the bridging ligand). They can also be used to categorize the systems according to the position of the bridge state above or below the usual mixed valence states.[40] Finally, they can explain the number of intervalence bands and the evolution of the intervalence and charge transfer bands.[33] Thus they convey more information than 2D diagrams made of parabolas, which are actually slices in the more complete 3D diagrams.

4.2. Quantitative models

In quantitative treatments, one tries to describe the complete system by advanced quantum mechanical methods (ideally *ab initio*), without trying to separate the structure into subunits. The main output is the total energy, and in some cases a geometry optimization is performed, in order to determine if the system is fully delocalized (class III - symmetrical ground state structure) or partly localized (class II or even I - unsymmetrical ground state structure). Due to space limitation, we do not treat here semiempirical methods (Extended Hückel, AM1, etc…) although their explanatory power is remarkable. We consider only high level methods based on wavefunctions or DFT. The following is inspired by the recent review by Kaupp.[41]

Historically, the earlier methods were based on wavefunctions, *i.e. ab initio* SCF molecular orbital methods, for instance CASSCF (Complete Active State Self-Consistent Field), with post-treatment in order to take into account dynamic correlation. However these methods tend to exaggerate localization as mentioned in section 3.1 of[41]. Success in reproducing the intervalence transition of the Creutz-Taube ion has been achieved by Bolvin[42] using the CASSCF/CASPT2 method (PT2 is a post-treatment by second-order perturbation theory). An interesting spin-off of wavefunction methods is the possibility to evaluate the electronic coupling parameter between diabatic states (if the system can be properly decomposed in fragments): using Koopmans theorem, V_{ab} can be obtained from the energy difference between two orbitals of different symmetries (g and u for a centrosymmetric system), these orbitals being computed for the parent homovalent system.[43]

Wavefunction-based methods are however too heavy for treating large structures. Thus the most popular methods are now DFT-based, because they use a single-determinant description, at a lower computational cost. The difficulty is however transferred on the choice of the best functional. Using the most common functionals, such as B3LYP introduces a bias towards delocalized electronic structures as explained in section 3.2 of[41]. The situation has improved recently with the setting up of a reliable protocol based on the BLYP35 functional, with in addition a treatment of the surrounding solvent by the COSMO model (a model describing the solvent as a dielectric continuum). The BLYP35 functional is a compromise hybrid, “35” meaning that it incorporates 35% of exact exchange, this percentage being adjusted to describe properly the state of localization/delocalization[41]. Recent uses of this protocol appear promising, in particular to design molecular wires with long-range charge delocalization.[44]

Although they do not play a central role in DFT, molecular orbitals (Kohn-Sham orbitals) can be computed. The shape and symmetry of these Kohn-Sham orbitals are very similar to those calculated by Hartree-Fock methods. In the story of the development of DFT, such orbitals were first ignored, but are now rehabilitated, because their physical meaning has been ascertained.[45] Thus they constitute a precious guide for chemists, allowing qualitative predictions of the effects of structure variation on the site properties, electronic coupling, etc… They also allow a pictorial description of electronic transitions in terms of electron jump between orbitals, if the TDDFT variant is used.

Finally, as mixed valence complexes are paramagnetic, DFT studies provide easily the repartition of spin density. Its distribution on the two sites gives information on the class II or III nature of the complex, provided of course that the geometrical structure has not been constrained.

Many mixed valence studies have used DFT to interpret experimental results, with compounds as diverse as Ru dimers with quinonoid bridge,[46] Ru dimers with diethynyl bridges,[40a] or other carbon-rich bridges,[19a, 47] Ru-amine-Ru systems,[9b] Ru trimers linked by cyanide bridges,[27a] etc… In most of the above papers, DFT is used in conjunction with Kohn-Sham orbitals to discuss spin density, electronic spectra, or EPR parameters, but generally

without theoretical determination of the ground state geometry, and in particular its symmetry.

Some studies address however this problem, which is particularly difficult because small energy differences are involved. Thus biferrocenium described with B3LYP functional, with geometry optimization, predicts surprisingly the correct localized nature of the ground state[48] ("surprisingly" because B3LYP has the reputation to favor a delocalized situation). However, as mentioned by Costuas *et al*,[40b] in many cases DFT uses a symmetrical structure for the initial electronic density, and this symmetry can be artefactually retained in the final result. A careful procedure with different starting symmetries is thus necessary.

For predicting the true symmetry, the combination of BLYP35 with COSMO for the solvent seems to be of general purpose. This combination has been first tested on organic mixed valence, with triphenylamine end groups, and later extended to relatively simple inorganic mixed valence systems with diethynylphenyl or pyrazine bridges, with an exploration of the possible symmetry breakings.[49]

Another tough problem is raised by the flexible nature of many mixed valence systems. Except for very small ligands, there is in particular a possibility of internal twisting changing dramatically the degree of electronic interaction between subunits at a low energy cost. This is notably the case for all-carbon bridges containing ethynyl groups. The importance of this effect has been stressed by Low.[21c] For instance for a mixed valence compound bridged by diethynylanthracene, the rotation of the anthracene unit could change the balance between metal-to-bridging ligand and metal-to-metal (intervalence) transitions.[40a]. For a homovalent dimer with M_2(acetate)$_4$ type of terminal unit, when the bridging ligand is a terephthalate (a phenylene with two acetates in para position) or a tetrasubstituted terephthalate, the ligand can present a planar or twisted conformation, according to the nature of the substituents (H4, F4, Cl4). This is experimentally evidenced by changes in the M_2 to π^* MLCT transition, and theoretically explained by DFT (B3LYP) calculations.[7a]

But the more recent BLYP35/COSMO association allows an in-depth exploration of the potential energy surface as a function of pertinent angles.[49] When the potential energy landscape is shallow, several conformations can be thermally populated, with consequences on the intervalence band profile and the vibrational spectra observed experimentally. Note that such studies could help understanding some experiments made with nanojunctions filled with phenylethynyl benzene molecules for which the exact conformation is difficult to determine.[21c]

5. Conclusion

The last 15 years have shown the richness and vitality of the domain of molecular mixed valence compounds. There is a growing interest on polymetallic end groups, which can bring specific advantages such as increased couplings, a better resolution of intervalence transitions, or an easier monitoring of the intramolecular electron transfer rate. From the point of view of bridging ligands, considerable progress has been achieved to understand the role of non-innocent bridging ligands. This was necessary since the most efficient in relaying the electronic interaction between remote sites are those for which there is an important mixing of metal and ligand levels, that is precisely the non-innocent ones ! The usual challenges of long-distance intervalence transfer and molecular switching have carried on. A new category, cross-conjugated ligands, has appeared, making the link with quantum interference concepts and the domain of molecular nanojunctions.

Theoretical treatments span a wide range, from simple qualitative models (simple but heuristically useful !) to quantitative models based on *ab initio* or quasi *ab initio* methods. The progress of DFT based methods is impressive and its use has generalized. However it is

important that such methods are coupled to a careful geometrical optimization, to address the question of the symmetry of the ground state and its electronic structure. But the task is huge, because as more and more geometrical degrees of freedom as considered, the potential energy hypersurface becomes more and more difficult to visualize. More than ever, a pertinent compromise must be searched between accuracy and understanding.

References

[1] (a) J.-P. Launay, *Chem. Soc. Rev*. **2001**, *30*, 386-397. (b) K. D. Demadis, C. M. Hartshorn, T. J. Meyer, *Chem. Rev*. **2001**, *101*, 2655-2685. (c) B. S. Brunschwig, C. Creutz, N. Sutin, *Chem. Soc. Rev*. **2002**, *31*, 168-184. (d) D. M. D'Alessandro, F. R. Keene, *Chem. Soc. Rev*. **2006**, *35*, 424-440. (e) P. Aguirre-Etcheverry, D. O'Hare, *Chem. Rev*. **2010**, *110*, 4839-4864. (f) A. Hildebrandt, H. Lang, *Organometallics* **2013**, *32*, 5640-5653. (g) W. Kaim, B. Sarkar, *Coord. Chem. Rev*. **2013**, *257*, 1650-1659. (h) J.-P. Launay, M. Verdaguer, *Electrons in Molecules (2nd Ed),* Oxford University Press, **2018**, Chapter 3.

[2] N. I. Gumerova, A. Rompel, *Nature Reviews Chemistry* **2018**, *2*, 0112.

[3] H. Lang, R. Packheiser, B. Walfort, *Organometallics* **2006**, *25*, 1836-1850. T. C. Stamatatos, B. S. Luisi, B. Moulton, G. Christou, *Inorg. Chem*. **2008**, *47*, 1134-1144. S.-I. Ohkoshi, H. Tokoro, *Acc. Chem. Res*. **2012**, *45*, 1749-1758.

[4] A. F. Wang, C. Ornelas, D. Astruc, P. Hapiot, *J. Am. Chem. Soc*. **2009**, *131*, 6652-6653. D. Astruc, A. Rapakousiou, Y. L. Wang, R. Djeda, A. Diallo, J. Ruiz, C. Ornelas, *J. Coord. Chem*. **2014**, *67*, 3809-3821.

[5] S. Flores-Torres, G. R. Hutchison, L. J. Soltzberg, H. D. Abruna, *J. Am. Chem. Soc*. **2006**, *128*, 1513-1522. G. Givaja, P. Amo-Ochoa, C. J. Gomez-Garcia, F. Zamora, *Chem. Soc. Rev*. **2012**, *41*, 115-147. K. Uemura, *Dalton Trans*. **2017**, *46*, 5474-5492.

[6] (a) R. A. Marcus, *Ann. Rev. Phys. Chem*. **1964**, *15*, 155. (b) G. C. Allen, N. S. Hush, *Progr. Inorg. Chem*. **1967**, *8*, 357. (c) M. B. Robin, P. Day, *Adv. Inorg. Chem. Radiochem*. **1967**, *10*, 267.

[7] (a) P. J. Low, N. J. Brown, *J. Clust. Sci.* **2010**, *21*, 235-278. (b) R. F. Winter, *Organometallics* **2014**, *33*, 4517-4536.

[8] J.-P. Launay, *Coord. Chem. Rev*. **2013**, *257*, 1544-1554.

[9] (a) J.-P. Djukic, J.-B. Sortais, L. Barloy, M. Pfeffer, *Eur. J. Inorg. Chem*. **2009**, 817-853. (b) Y.-W. Zhong, Z.-L. Gong, J.-Y. Shao, J. Yao, *Coord. Chem. Rev*. **2016**, *312*, 22-40. (c) J.-Y. Shao, Z.-L. Gong, Y.-W. Zhong, *Dalton Trans*. **2018**, *47*, 23-29.

[10] C. Patoux, J.-P. Launay, M. Beley, S. Chodorowski-Kimmes, J.-P. Collin, S. James, J.-P. Sauvage, *J. Am. Chem. Soc*. **1998**, *120*, 3717-3725.

[11] (a) M. H. Chisholm, N. J. Patmore, *Acc. Chem. Res*. **2007**, *40*, 19-27. (b) B. J. Lear, M. H. Chisholm, *Inorg. Chem*. **2009**, *48*, 10954-10971. (c) M. H. Chisholm, B. J. Lear, *Chem. Soc. Rev*. **2011**, *40*, 5254-5265. (d) M. H. Chisholm, *Coord. Chem. Rev*. **2013**, *257*, 1576-1583. (e) H. Lei, X. Xiao, M. Meng, T. Cheng, Y. Shu, Y. N. Tan, C. Y. Liu, *Inorg. Chim. Acta* **2015**, *424*, 63-74.

[12] (a) T. Ren, *Organometallics* **2005**, *24*, 4854-4870. (b) H. Zhu, S. J. Pookpanratana, J. Y. Bonevich, S. N. Natoli, C. A. Hacker, T. Ren, J. S. Suehle, C. A. Richter, Q. Li, *ACS Appl. Mat. Interfaces* **2015**, *7*, 27306-27313.

[13] S. D. Glover, J. C. Goeltz, B. J. Lear, C. P. Kubiak, *Coord. Chem. Rev*. **2010**, *254*, 331-345.

[14] (a) W. Kaim, G. K. Lahiri, *Angew. Chem. Int. Ed*. **2007**, *46*, 1778-1796. (b) S. Maji, B. Sarkar, S. M. Mobin, J. Fiedler, F. A. Urbanos, R. Jimenez-Aparicio, W. Kaim, G. K. Lahiri, *Inorg. Chem*. **2008**, *47*, 5204-5211. (c) W. Kaim, *Inorg. Chem*. **2011**, *50*, 9752-9765. (c) A. S. Hazari, A. Indra, G. K. Lahiri, *RSC Adv*. **2018**, *8*, 28895-28908.

[15] M. L. Naklicki, R. J. Crutchley, *J. Am. Chem. Soc*. **1994**, *116*, 6045-6046.

[16] M. Fabre, J. Jaud, M. Hliwa, J.-P. Launay, J. Bonvoisin, *Inorg. Chem*. **2006**, *45*, 9332-9345.

[17] (a) M. L. Naklicki, S. I. Gorelski, W. Kaim, B. Sarkar, R. J. Crutchley, *Inorg. Chem*. **2012**, *51*, 1400-1407. (b) M. M. M. Choudhuri, W. Kaim, B. Sarkar, R. J. Crutchley, *Inorg. Chem*. **2013**, *52*, 11060-11066.

[18] M. A. Ansari, A. Mandal, A. Paretzki, K. Beyer, W. Kaim, G. K. Lahiri, *Inorg. Chem*. **2016**, *55*, 12357-12365.

[19] (a) K. Costuas, S. Rigaut, *Dalton Trans*. **2011**, *40*, 5643-5658. (b) P. A. Schauer, P. J. Low, *Eur. J. Inorg. Chem.* **2012**, 390-411. (c) J.-F. Halet, C. Lapinte, *Coord. Chem. Rev.* **2013**, *257*, 1584-1613. (d) Y. Tanaka, M. Akita, *Coord. Chem. Rev*. **2019**, *388*, 334-342.

[20] T. L. Gianetti, G. Nocton, S. G. Minasian, N. Kaltsoyannis, A. L. D. Kilcoyne, S. A. Kozimor, D. K. Shuh, T. Tyliszczak, R. G. Bergman, J. Arnold, *Chem. Sci*. **2015**, *6*, 993-1003.

[21] (a) M. Akita, Y. Tanaka, C. Naitoh, T. Ozawa, N. Hayashi, M. Takeshita, A. Inagaki, M.-C. Chung, *Organometallics* **2006**, *25*, 5261-5275. (b) Special issue of *Polyhedron*, **2015**, *86*, 1-166 dedicated to C. Lapinte. (c) P. J. Low, *Coord. Chem. Rev*. **2013**, *257*, 1507-1532.

[22] Z. Cao, B. Xi, D. S. Jodoin, L. Zhang, S. P. Cummings, Y. Gao, S. F. Tyler, P. E. Fanwick, R. J. Crutchley, T. Ren, *J. Am. Chem. Soc*. **2014**, *136*, 12174-12183.

[23] M. Magoga, C. Joachim, *Phys. Rev. B* **1997**, *56*, 4722-4729.

[24] B. Xi, I. P-C. Liu, G.-L. Xu, M. M. R. Choudhuri, M. C. DeRosa, R. J. Crutchley, T. Ren, *J. Am. Chem. Soc*. **2011**, *133*, 15094-15104.

[25] M. Fabre, J. Bonvoisin, *J. Am. Chem. Soc*. **2007**, *129*, 1434-1444.

[26] G. N. Newton, M. Nihei, H. Oshio, *Eur. J. Inorg. Chem*. **2011**, 3031-3042.

[27] (a) Y.-Y. Yang, X.-Q. Zhu, S.-M. Hu, S.-D. Su, L. T. Zhang, Y.-H. Wen, X.-T. Wu, T.-L. Sheng, *Angew. Chem. Int. Ed*. **2018**, *57*, 14046-14050. (b) X. Ma, C.-S. Lin, S.-M. Hu, C.-H. Tan, Y.-H. Wen, T.-L. Sheng, X.-T. Wu, *Chem. Eur. J.* **2014**, *20*, 7025-7036.

[28] (a) M. I. Bruce, A. Burgun, M. A. Fox, M. Jevric, P. J. Low, B. K. Nicholson, C. R. Parker, B. W. Skelton, A. H. White, N. N. Zaitseva, *Organometallics*, **2013**, *32*, 3286-3299. (b) W. P. Forrest, M. M. R. Choudhuri, S. M. Kilyanek, S. N. Natoli, B. M. Prentice, P. E. Fanwick, R. J. Crutchley, T. Ren, *Inorg. Chem*. **2015**, *54*, 7645-7652. (c) R. Makhoul, J. B. G. Gluyas, K. B. Vincent, H. Sahnoune, J.-F. Halet, P. J. Low, J.-R. Hamon, C. Lapinte, *Organometallics*, **2018**, *37*, 4156-4171. (d) Y. Fan, H.-M. Li, G.-D. Zou, X. Zhang, Y.-L. Pan, K.-K. Cao, M. L. Zhang, P.-L. Ma, H.-T. Lu,

Organometallics, **2017**, *36*, 4278-4286. (e) E. Goransson, R. Emmanuelsson, K. Jorner, T. F. Markle, L. Hammastrom, H. Ottosson, *Chem. Sci*. **2013**, *4*, 3522-3532.

[29] (a) C. Patoux, C. Coudret, J.-P. Launay, C. Joachim, A. Gourdon, *Inorg. Chem*.**1997**, *36*, 5037-5049. (b) H. Gao, S. Mallick, L. Cao, M. Meng, T. Cheng, H. W. Chen, C. Y. Liu, *Chem. Eur. J*. **2019**, *25*, 3930-3938. (c) A. A. Kocherzhenko; L. D. A. Siebbeles, F. C. Grozema, *J. Phys. Chem. Lett*. **2011**, *2*, 1753-1756. (d) K. B. Vincent, Q. Zeng, M. Parthey, D. S. Yufit, J. A. E. Howard, F. Hartl, M. Kaupp, P. J. Low, *Organometallics*, **2013**, *32*, 6022-6032.

[30] (a) G. C. Solomon, D. Q. Andrews, R. P. Van Duyne, M. A. Ratner, *J. Am. Chem. Soc*, **2008**, *130*, 7788-7789. (b) Y. Tsuji, R. Hoffmann, *Angew. Chem. Int. Ed*. **2014**, *53*, 4093-4097. (c) ref [1h], p 482. (d) J.-P. Launay, *Polyhedron*, **2015**, *86*, 151-166.

[31] (a) O. S. Wenger, *Chem. Soc. Rev*. **2012,** *41*, 3772-3779. (b) S. Fraysse, C. Coudret, J.-P. Launay, *Eur. J. Inorg. Chem*. **2000**, 1581-1590. (c) K. Motoyama, H. Li, M. Hatakeyama, S. Yokojima, S. Nakamura, M. Akita, *Dalton Trans*. **2011**, *40*, 10643-10657. (d) Y. F. Liu, C. Lagrost, K. Costuas, N. Tchoubar, H. Le Bozec, S. Rigaut, *Chem. Comm*. **2008**, 6117-6119. (e) A. Escribano, T. Steenbock, C. Herrmann, J. Heck, *ChemPhysChem* **2016**, *17*, 1881-1894. (f) J. P. Calupitan, T. Nakashima, Y. Hashimoto, T. Kawai, *Chem. Eur. J*. **2014**, *22*, 10002-10008. (g) G. Guirado, C. Coudret, J.-P. Launay, *J. Phys. Chem. C* **2007**, *111*, 2770-2776. (h) Y. Tanaka, T. Ishisaka, T. Koike, M. Akita, *Polyhedron* **2015**, *86*, 105-110.

[32] See for instance the rich behavior with 6 states exhibited by a binuclear nickel compound linked by a terpyridyl-containing ligand: B. Doistau, L. Benda, J.-L. Cantin, L.-M. Chamoreau, E. Ruiz, V. Marvaud, B. Hasenknopf, G. Vives, *J. Am. Chem. Soc*. **2017**, *139*, 9213-9220. According to the different stimulations, the molecule can adopt either an extended or folded configuration (tweezer effect), but the nickel terminal sites are not adapted to mixed valence studies.

[33] S. D. Glover, C. P. Kubiak, *J. Am. Chem. Soc*. **2011**, *133*, 8721-8731.

[34] D. M. D'Alessandro, F. R. Keene, *Chem. Rev*. **2006**, *106*, 2270-2298. J. F. Endicott, Y.-J. Chen, *Coord. Chem. Rev*. **2013**, *257*, 1676-1698.

[35] Note that even for a two-site system, it could be necessary to rely on 3D diagrams if the two combinations of vibrational coordinates localized on each site are taken into account. This is developed in a "vibronic PKS model revisited": A. Pali, B. Tsukerblat, J. M. Clemente-Juan, S. M. Aldoshin, *J. Phys. Chem A* **2015**, *119*, 9844-9856.

[36] M. J. Ondrechen, J. Ko, L. J. Root, *J. Phys. Chem*. **1984**, *88*, 5919-5923. M. J. Ondrechen, J. Ko, L.-T. Zhang, *J. Am. Chem. Soc*. **1987**, *109*, 1672-1676.

[37] I. B. Bersuker, S. A. Borsch, I. F. Chibotaru, *Chem. Phys*. **1989**, *136*, 379-384.

[38] C. Lambert, G. Noll, J. Schelter, *Nat. Mater*. **2002**, *1*, 69-73. C. Lambert, S. Amthor, J. Schelter, *J. Phys. Chem. A*, **2004**, *108*, 6474-6486.

[39] J.-P. Launay, C. Coudret, C. Hortholary, *J. Phys. Chem. B* **2007**, *111*, 6788-6797.

[40] (a) M. A. Fox, B. Le Guennic, R. L. Roberts, D. A. Brue, D. S. Yufit, J. A. K. Howard, G. Manca, J.-F. Halet, F. Hartl, P. J. Low, *J. Am. Chem. Soc*. **2011**, *133*, 18433-18446. (b) K. Costuas, O. Cador, F. Justaud, S. Le Stang, F. Paul, A. Monari, S. Evangelisti, L. Toupet, C. Lapinte, J.-F. Halet, *Inorg. Chem*. **2011**, *50*, 12601-12622.

[41] M. Parthey, M. Kaupp, *Chem. Soc. Rev*. **2014**, *43*, 5067-5088.

[42] H. Bolvin, *Inorg. Chem*. **2007**, *46*, 417-427.

[43] J.-P. Malrieu, R. Caballol, C. J. Cazado, C. de Graaf, N. Guihery, *Chem. Rev*. **2014**, *114*, 429-492.

[44] S. Kroncke, C. Herrmann, *J. Chem. Theory Comput*. **2019**, *15*, 165-177.

[45] R. Stowasser, R. Hoffmann, *J. Am. Chem. Soc*. **1999**, *121*, 3414-3420. E. J. Baerends, O. V. Gritsenko, R. van Meer, *Phys. Chem. Chem. Phys*. **2013**, *15*, 16408-16425.

[46] S. Ghumaan, S. Mukherjee, S. Kar, D. Roy, S. M. Mobin, R. B. Sunoj, G. K. Lahiri, *Eur. J. Inorg. Chem*. **2006**, 4426-4441.

[47] C. Olivier, K. Costuas, S. Choua, V. Maurel, P. Turek, J.-Y. Saillard, D. Touchard, S. Rigaut, *J. Am. Chem. Soc*. **2010**, *132*, 5638-5651.

[48] R. G. Hadt, V. N. Nemykin, *Inorg. Chem*. **2009**, 48, 3982-3992.

[49] M. Parthey, J. B. G. Gluyas, M. A. Fox, P. J. Low, M. Kaupp, *Chem. Eur. J*. **2014**, *20*, 6895-6908.

Figures captions

Fig 1. General structure of the mixed valence compounds considered in this review. M_n designates a terminal site consisting of either a monometallic or a polymetallic center (n = 1-3)

Fig 2. Marcus-Hush curves for a two-site system. Left ; class II, two minima on the lowest potential energy curve. Right : class III, only one minimum. E is the potential energy of the system, λ the reorganization energy, V_{ab} the electronic interaction.between the two localized electronic states. The Q coordinate corresponds to an asymmetric combination of the breathing modes on each subunit. Strictly speaking, it encompasses a solvent coordinate (not shown here).

Fig 3. Examples of cyclometallated structures. (a) derived from $Ru(bpy)_3$, by replacement of a bipyridine ligand by a phenylpyridine. (b) derived from $Ru(terpy)_2$ by replacement of a nitrogen atom either on a central or a lateral group of terpyridine. The plain arrow show the direction of bonding with the bridging ligand.

Fig 4. Structures of bimetallic terminal groups. (a) based on $M_2(acetate)_4$ one of the acetate group being substituted in the plain arrow direction. M atoms are linked by a quadruple bond. (b) based on the $Ru_2(ap)_4$ structure, ap = 2-anilinopyridinate or derivative. The Ru-Ru bond orde is 2.5. Note that this terminal group links by one end only.

Fig 5. Structure of the $[Ru_3O(acetate)_6(CO)L_2]$ terminal group. One of the L ligand can be a bridging ligand (pyrazine, 4,4'-bipyridine or derivatives).

Fig 6. General structure with a non-innocent bridging ligand (BL), showing the possible states of the system when one electron is added or removed to the homovalent form.
(A) oxidation bearing on the terminal sites, generating a mixed-valence system; (B) oxidation bearing on the bridging ligand, generating a homovalent form with an oxidized ligand. Note that interrmediate cases are possible by mixing resonant forms.

Fig 7. Structures of (a) the dicyanamido benzene ligand and (b) extended dicyanamido ligands.

Fig 8. Mesomeric forms favored by oxidation for (a) cyanamido ligand; (b) carbon-rich alkynyl ligand. Note the difficulty in the carbon-rich case to assign a precise location for the positive charge.

Fig 9. Central part of a cross-conjugated bridging ligand. (a) penta-diyn-3-one. 'b) *gem*-diethynylethene.

Fig 10. Central part of a typical switching ligand based on diethienylethene, showing the initial open form (OFF) and the photo cyclized closed form (ON).

Fig 11. Overview of the different theoretical descriptions : (a) orbital energies; (b) Marcus-Hush curves for two states; (c) Marcus-Hush curves for three states; (d) 3D surfaces with paraboloids for three states; (e) complete computation (wave-function method or DFT), for different geometries.

Fig1

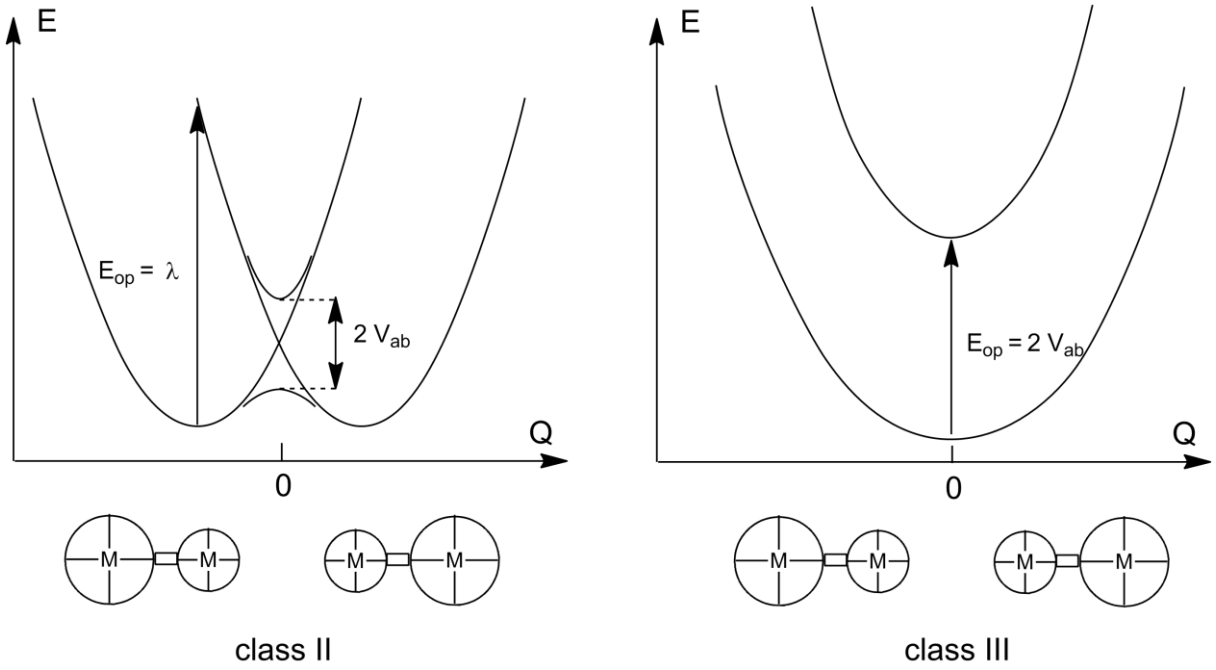

Fig 2

(a)

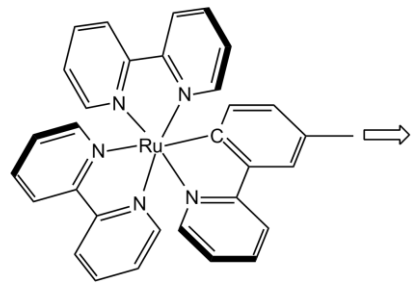

(b)

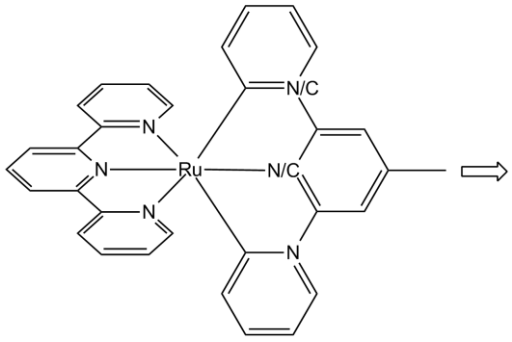

Fig 3

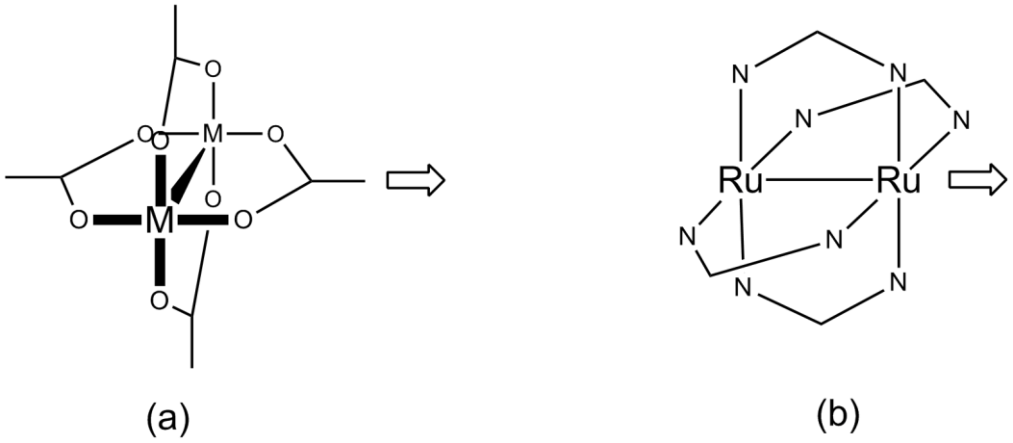

Fig 4

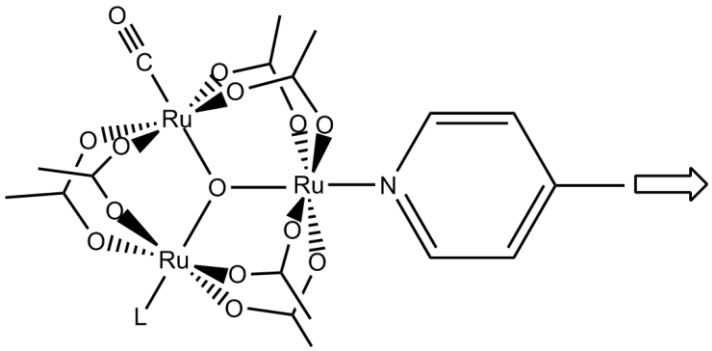

Fig 5

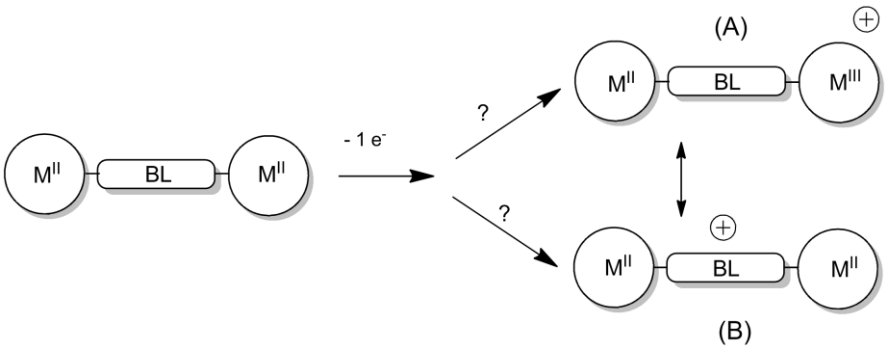

Fig 6

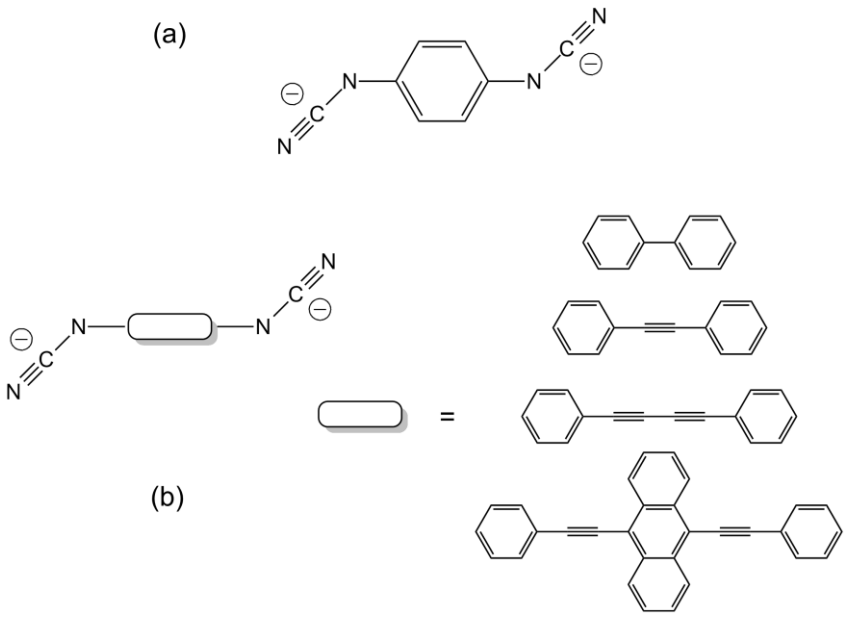

Fig 7

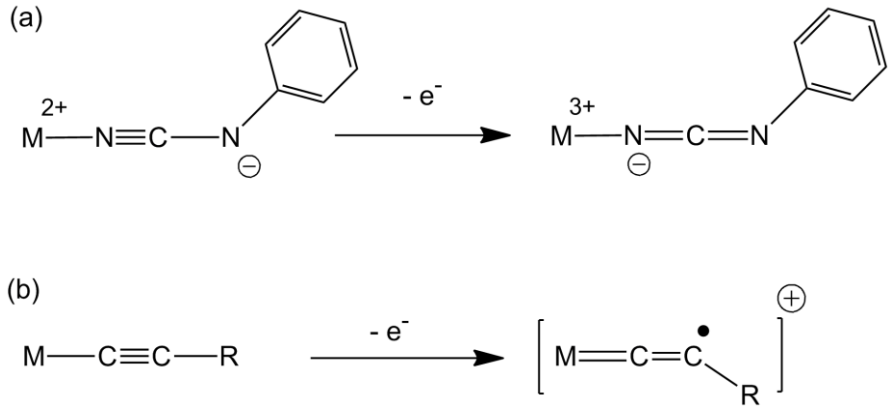

Fig 8

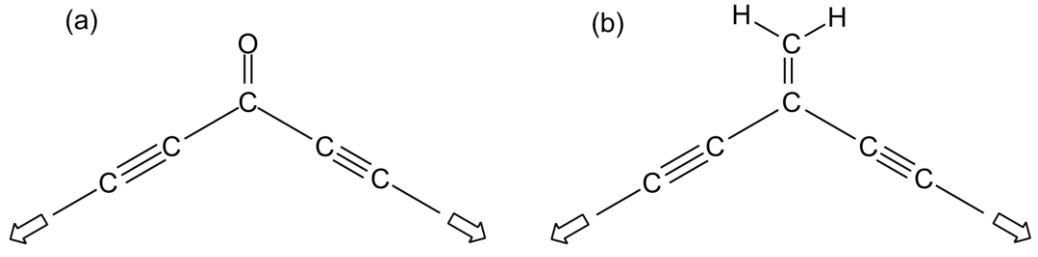

Fig 9

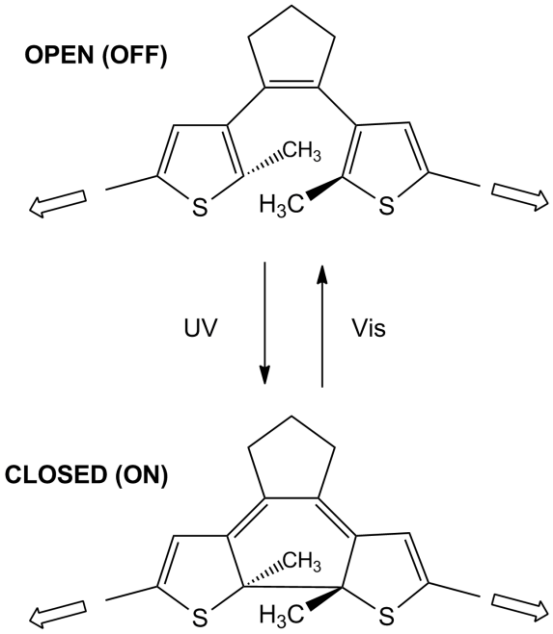
OPEN (OFF)
CH3
H3C
S
S
UV
Vis
CLOSED (ON)
CH3
H3C
S
S

Fig 10

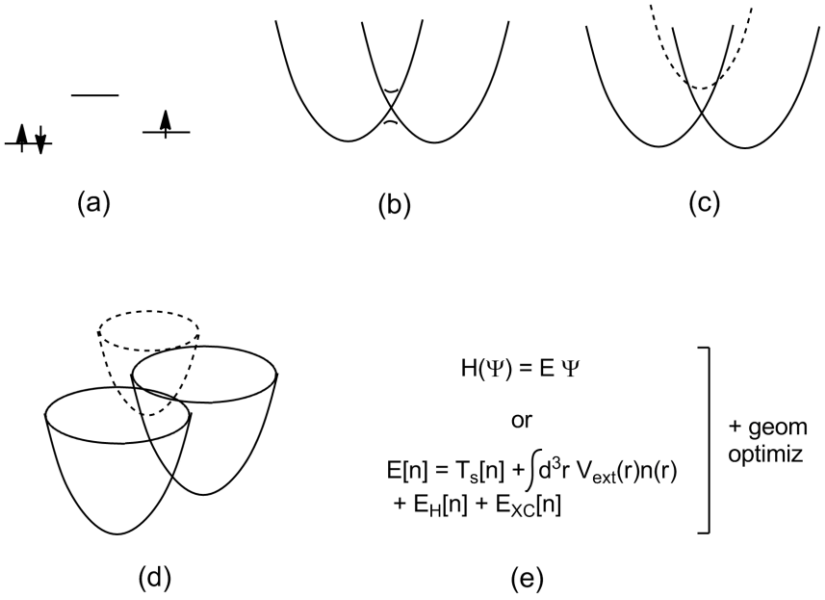
(a)
(b)
(c)
(d)
H(Ψ) = E Ψ
or
E[n] = Ts[n] + ∫d3r Vext(r)n(r)
+ EH[n] + EXC[n]
+ geom
optimiz
(e)

Fig 11

Illustrated Abstract

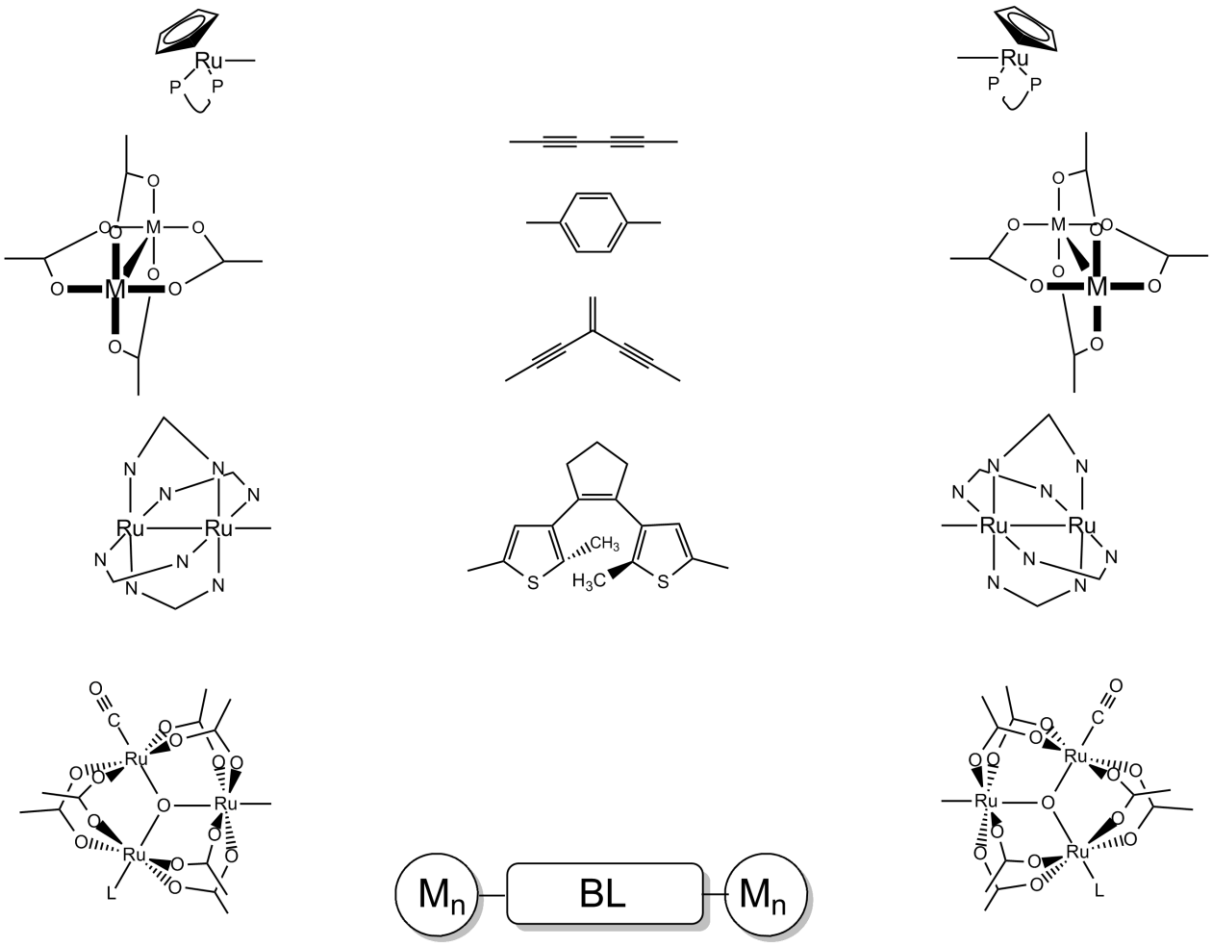

A large variety of molecular mixed valence compounds are reviewed, combining diverse terminal groups (mono- or polymetallic) with bridging ligands exhibiting special properties for electron transfer and switching. Theoretical descriptions, from simple qualitative models to quantitative ones, are discussed.